Controllable Excitation of Surface Plasmons in End-to-Trunk Coupled Silver Nanowire Structures

2012 Chinese Phys. Lett. 29 077302

(http://iopscience.iop.org/0256-307X/29/7/077302)

CHIN. PHYS. LETT. Vol. 29, No. 7 (2012) 077302

Controllable Excitation of Surface Plasmons in End-to-Trunk Coupled Silver Nanowire Structures *

ZHU Yin(朱殷), WEI Hong(魏红), YANG Peng-Fei(杨鹏飞), XU Hong-Xing(徐红星)**

Beijing National Laboratory for Condensed Matter Physics and Institute of Physics, Chinese Academy of Sciences, P.O. Box 603-146, Beijing 100190

(Received 5 April 2012)

In branched nanowire structures, the controllable excitation of surface plasmons is investigated by both experiments and simulations. By focusing the excitation light at the junction between the main wire and the branch wire, surface plasmons can be selectively launched to propagate to different output terminals, depending on the polarization of the excitation light. The parameters influencing the plasmon excitation and thus emission behavior are investigated, including the branch angle, the position of the branch and the nanowire radius. The different polarization dependence of the output light is determined by the surface plasmon modes selectively excited in the junction through end-excitation or/and gap-excitation manners. For the branch wire, when the branch angle is small, the end-excitation is dominant, which makes the branched wire behave like an individual nanowire. With the increase of the branch angle, the coupling between the branch wire end and the primary wire trunk is increased, which influences the plasmon excitation in the branch wire as evidenced by the rotation of the polarization angle for maximum output. For the primary wire, the SP excitation is dependent on the branch angle, position of the junction along the primary wire, and the radii of the nanowires. The results may be important for the design of a controllable surface plasmon launcher, one of the functional components in surface-plasmon-based nanophotonic circuits.

PACS: 73.20.Mf, 42.25.Ja, 78.67.Uh DOI: 10.1088/0256-307X/29/7/077302

The manipulation of light at the nanometer scale based on surface plasmons (SPs) has attracted intensive interest from many different fields. Metal nanostructures which support SP resonances show many valuable properties and are used in various applications, such as surface-enhanced spectroscopy,[1,2] surface plasmon resonance sensing,[3,4] SP-assisted optical tweezers,[5,6] nanolasers,[7] nanophotonic devices and circuits,[8–12] and quantum information processing.[13,14] In one-dimensional metal nanostructures, SPs can propagate along the waveguide with tight confinement of the local electromagnetic field in the transverse dimension. Propagating SPs have been investigated in different waveguide structures, of which crystalline silver nanowires attract special attention.[15–22] The emission direction and polarization,[23–25] loss caused by the metal and the substrates,[26–28] and group velocity[29,30] have been studied. Recently, SP interferences have been successfully used to control and modulate the propagating plasmons in nanowire networks, and binary logic gates can be built.[10,31] Hence, the silver nanowires are good elements for the demonstration of SP-based nanophotonic circuits. To build functional plasmonic circuits, the controllable excitation and distribution of SPs in a nanowire network is an inevitable issue.

In this Letter, we investigate the SP excitation in three-terminal nanowire structures composed of two Ag nanowires coupled in an end-to-trunk configuration. Excitation laser light is focused at the connecting junction of two wires to generate propagating SPs, which couple out at the output terminals as photons. Experimental results show that the SP excitation is strongly dependent on the polarization of the incident light. For the branch wire, the plasmons can be efficiently launched when the incident light is polarized along this wire. For the main wire, the generation of SPs shows more complex behavior, dependent on the geometrical details of the branched wire structure. Electromagnetic simulations using the finite element method (FEM) are also performed to investigate the polarization dependence of the output light. The influences of different nanowire structure geometries on the SP emission behaviors are studied.

The crystalline Ag nanowires were synthesized using a reported protocol.[32] Then an ethanol suspension of Ag nanowires was spin-coated on glass slides patterned with indexed grids, which can help to find the same structure with both an optical microscope and a scanning electron microscope (SEM). Branched nanowire structures randomly formed can be found on the sample. The mean diameter of the Ag nanowire is about 280 nm, and the lengths range from 5 to 20 μm. The optical measurements were performed based on an upright microscope. The laser light of 633 nm wavelength was focused on the junction of the branched nanowire structure through a 100×(NA 0.95) objective. The back-scattered light was collected by the same objective and directed to a CCD camera to record the images. The polarization of the laser light was controlled by a half-wave plate. The polarization angle is defined as the angle between the polarization

*Supported by the National Natural Science Foundation of China under Grant Nos 10625418, 10874233, 11004237 and 11134013, the National Basic Research Program of China under Grant No 2009CB930700, and the Knowledge Innovation Project of Chinese Academy of Sciences (KJCX2-EW-W04).

**Corresponding author. Email: hxxu@iphy.ac.cn

direction and the branch wire. In the branched structures, the three terminals are separated far enough from the junction, which guarantees that the output light from the three terminals can be detected without the interference from the excitation light at the junction.

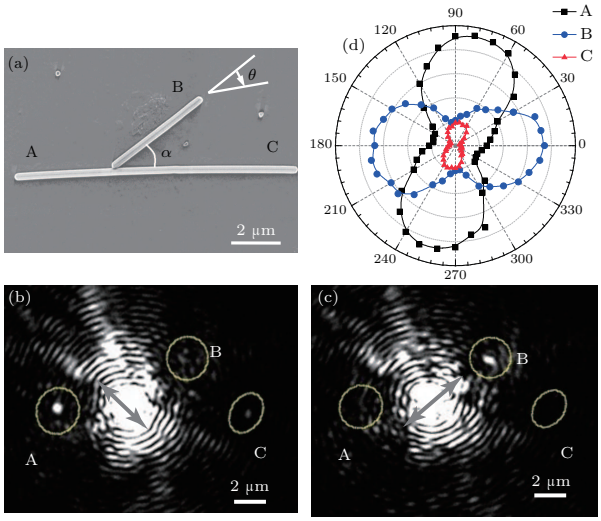

Fig. 1. (a) SEM image of one end-to-trunk coupled nanowire structure, (b,c) the optical images for the polarization angle of 80° (c) and 0° (d) as shown by the grey arrows. (d) The intensity from the three output terminals A (black), B (blue) and C (red) at different polarization angles.

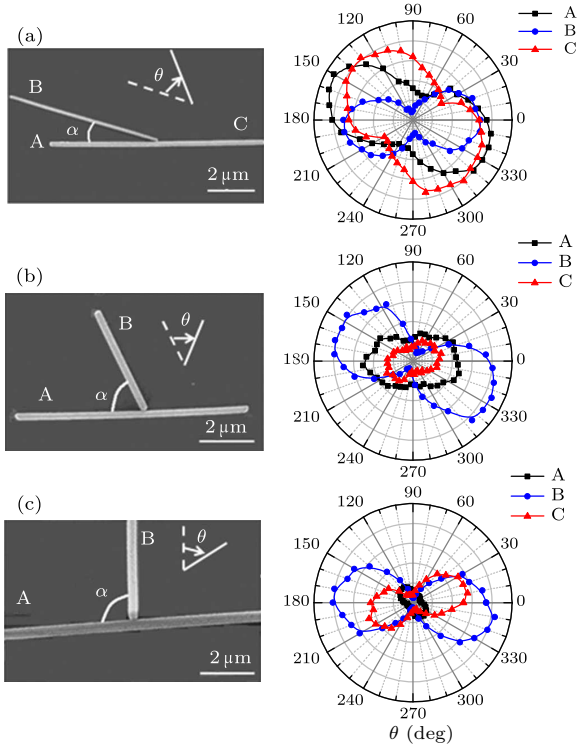

Fig. 2. SEM images and polarization dependent output intensity at three terminals A (black), B (blue) and C (red) for three different end-to-trunk coupled nanowire structures.

Figure 1(a) shows the SEM image of an end-to-trunk coupled Ag nanowire structure. The diameter of the branch wire (short one) is 303 nm and the length is 4.62 μm. For the main wire, the diameter and length are 289 nm and 11.6 μm, respectively. The angle between the two nanowires is about 37°. When the connecting junction is illuminated by the 633 nm wavelength laser light, SPs are launched not only in the branch wire, but also in the main wire, which is evidenced by the light scattering at the nanowire terminals. The intensity of the scattered light at the three output terminals (A, B and C) strongly depends on the polarization of the laser light. Figures 1(b) and 1(c) show the scattering images under two different incident polarizations. As can be seen, for the polarization shown by the grey arrow in Fig. 1(b), the output intensity at terminal A is strong, while for the polarization shown in Fig. 1(c), the output intensity at terminal B is strong. The output intensity at the three terminals for different laser polarizations is plotted in Fig. 1(d). The output intensity of all the three terminals shows strong polarization dependence. For the branch wire, the output intensity at terminal B becomes maximal when the laser polarized along the branch wire ($\theta = 0°$). Meanwhile, the output intensity of terminals A and C is close to the minimum for this polarization. For an incident polarization of 80°, strong light emission is obtained at terminal A and the light emission at terminal B is weak, which means that the SPs are only efficiently launched in the main nanowire.

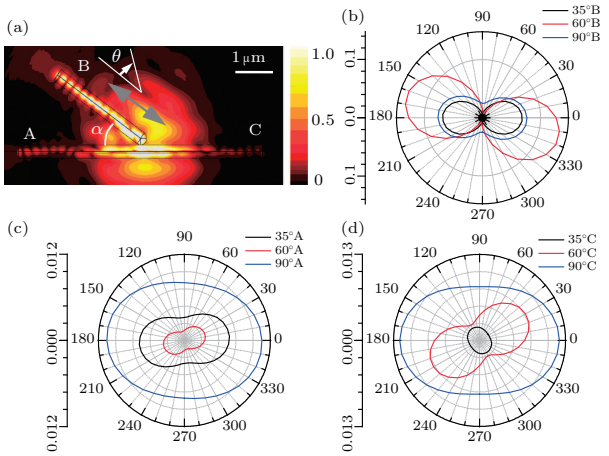

Fig. 3. (a) FEM simulation of electric field intensity distribution in an end-to-trunk coupled Ag nanowire structure excited by a Gaussian beam (beam waist 1 μm) at the junction. The coupling end of the branch wire (length L_b = 2.5 μm, radius R_b = 150 nm) capped the middle point of the main wire (length L_m = 6 μm, radius R_m = 150 nm) with the angle of 35° between the two wires. The polarization of the excitation light is parallel to the branch wire. (b–d) The incident polarization dependent intensity of the terminals B (b), A (c) and C (d) for the branch angle α of 35° (black), 60° (red) and 90° (blue).

In this structure, the polarization dependence of the output light at the branch wire terminal is the same as that of a single wire. Thus the excitation of SPs in the branch wire is mainly determined by the

nanowire end at the junction. We classify the SP generation manner at the nanowire end as end-excitation. For the main nanowire, the excitation of the plasmons happened at the wire trunk where adjacent nanowire exists. The coupling between the main wire and the branch wire enables the excitation of SPs in the main wire. We classify this kind SP excitation manner as gap-excitation. For this kind of excitation configuration, the wave vectors that can lead to the SP excitation are different from the end-excitation configuration. Depending on the detailed geometry of the gap, different plasmon modes are excited, which results in different polarization dependence of the output behavior of the main wire.

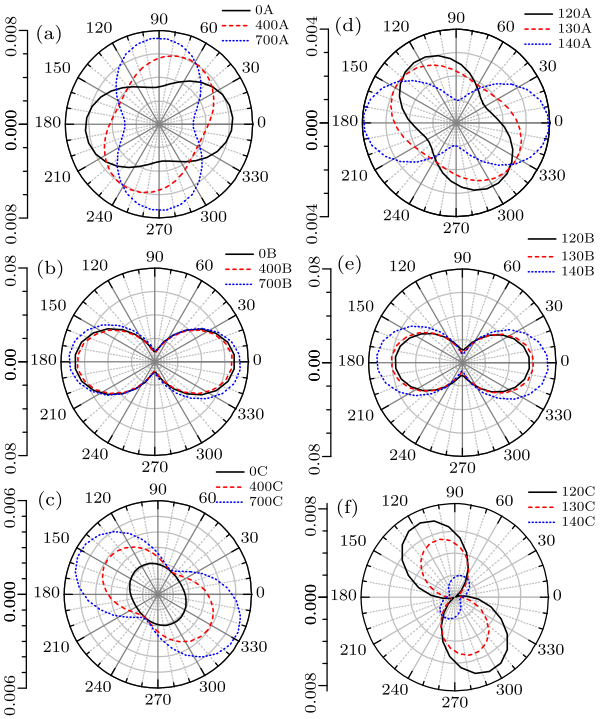

Fig. 4. FEM simulations of output intensity at three terminals in an end-to-trunk coupled Ag nanowire structure. The angle between the branch wire ($L_b = 2.5\,\mu$m, $R_b = 150$ nm) and the main wire ($L_m = 6\,\mu$m, $R_m = 150$ nm) is 35°. (a–c) The output intensity at terminals A (a), B (b) and C (c) for the junction at the middle of the main wire (black), moving 400 nm (red) and 700 nm (blue) right of the middle. (d–f) The output intensity at terminals A (d), B (e) and C (f) for the branch wire radius of 120 nm (black), 130 nm (red) and 140 nm (blue). The radius of the main wire is 150 nm. The junction is at the middle of the main wire.

We experimentally measured different branched nanowire structures and found the structure-dependent output behavior. Figure 2 shows three structures with different angles between the branch wire and the main wire, and different nanowire dimensions. For the gap-exciation of SPs in the main nanowires, the output intensity at terminals A and C shows different behaviors, due to the selective excitation of different plasmon modes in the junction. In addition, the diameter of the nanowire can also influence the modes that can be excited. However, the polarization dependence of the branch nanowire is less sensitive to the detailed nanostructure geometries. As can be seen in Figs. 2(a)–2(c), the output intensity at the branch terminal B becomes maximum when the laser polarization is parallel to the branch wire (Figs. 2(a) and 2(c)) or deviates little from the branch wire (Fig. 2(b)). The deviation of the polarization angle for maximum output at terminal B is about 20° in Fig. 2(b). This small rotation of the laser polarization is probably caused by the junction of narrow gap, which influences the excitation of plasmon modes by end-excitation configuration.

Simulations using the finite element method (COMSOL multiphysics) were performed to investigate the influence of the nanowire structure parameters on the polarization-dependent SP excitation. The simulated structure is composed of a main nanowire (6 μm length and 150 nm radius) and a branch wire (2.5 μm length and 150 nm radius). The excitation light was simulated by a polarized Gaussian beam (beam waist 1 μm), which was incident on the connecting junction of the branched structure. Figure 3(a) shows the near-field distribution when the excitation light was incident on the junction. SPs are generated by the laser illumination, which can be seen from the strong near-field distribution along the nanowire. The emission intensity at the output terminals is obtained by averaging the electric field intensity over the nanowire cross section. Figure 3(b) shows the dependence of the emission intensity at terminal B on the incident polarization angles for three different angles between the branch and the main nanowires. As can be seen, for different branch angles, the emission intensity at terminal B is always strongly dependent on the polarization of the laser light. For the branch angle of 35° and 90°, the emission intensity at terminal B is maximal when the polarization angle is 0° (the laser polarized parallel to the branch wire, black and green curves in Fig. 3(b)). While for the branch angle of 60°, the emission at terminal B is strongest when the polarization angle is −15° (red curve in Fig. 3(b)). Furthermore, the absolute emission intensity at terminal B for a branch angle of 60° is much stronger than those of branch angles 35° and 90°. The different behaviors for different branch angles can be understood by considering the excitation configurations. When the branch angle is small, e.g. 35°, the excitation of SPs in the branch wire is mainly determined by the end-excitation and the effect of the gap-excitation at the junction is small. With the increase of the branch angle, more of the branch wire end is coupled to the main wire trunk, and the contribution of gap-excitation is increased, which makes the polarization dependence behavior of the branch wire different from that of a single wire. The polarization angle corresponding to the maximum emission is −15°, which agrees well with the experimental data in Fig. 2(b). On the other hand, the gap-excitation configuration also improves the in-coupling efficiency for the plasmon excitation, thus stronger emission at the branch terminal B is observed. When the branch angle is increased to 90°, the symmetry of the gap determines

that the SP excitation efficiency at the junction is the highest when the laser light polarized along the branch wire. By comparing the three curves in Fig. 3(b), we can see that the green curve is less dependent on the incident polarization compared with the black and the red curves. To quantitatively evaluate the polarization dependence, we define the degree of polarization dependence $\rho = \frac{I_{\max}-I_{\min}}{I_{\max}+I_{\min}}$, where I_{max} is the maximum output intensity, $I_{\min}$ is the minimum output intensity. From the data in Fig. 3(b), we can obtain that the degrees of polarization dependence corresponding to the branch angles of 35°, 60° and 90° are 0.74, 0.89 and 0.52, respectively. The polarization dependence is weakest when the branch angle is 90°, and strongest when the branch angle is 60°. The asymmetric strong coupling between the branch wire end and the main wire trunk modifies the polarization dependence of the branch wire and improves the excitation efficiency for optimal incident polarization, and results in an output behavior strongly dependent on the polarization of the excitation light. Figures 3(c) and 3(d) show the output intensity at different incident polarization angles for three different branch angles. For both terminals of the main nanowire, the emission intensity is strongest when the branch angle is 90°. Although the degree of polarization dependence for the emission at terminal A and C is much smaller than that of terminal B, it is maximal when the branch angle is 60° (0.41 for terminal A and 0.51 for terminal C), and minimal when the branch angle is 90° for terminal A (0.15) and 35° for terminal C (0.14).

Besides the branch angle, the position of the connecting junction and the nanowire radius also influence the output behavior. Figures 4(a)–4(c) shows the simulated output intensity at the terminals A, B and C in the structure of branch angle 35°, for moving the coupling end of the branch wire from the middle point of the main nanowire to the right by 0 nm, 400 nm and 700 nm, respectively. The polarization dependence of the emission intensity at terminal A is sensitive to the movement of the branch wire. The polarizations corresponding to the maximum output are rotated anticlockwise. When the branch end is at the middle of the main wire, the emission intensity at terminal A is maximal when the laser polarization angle is $\theta = 10°$. With the branch moved 400 nm to the right, the emission at terminal A is strongest when $\theta = 60°$. When the branch is moved further to the right to the position of 700 nm away from the middle, the emission at terminal A is strongest when $\theta = 90°$. The maximal output intensity for the three different junctions is similar. For the output at terminal B, the intensity is highest when the laser polarized parallel to the branch wire ($\theta = 0°$). For the branch angle of 35°, the end-excitation is dominant for the plasmons in the branch wire, which is insensitive to the movement of the branch wire along the main wire and determines the maximum output intensity for $\theta = 0°$. For the terminal C, the maximum output intensity also rotates anticlockwise relative to the polarization angle as the branch wire is moved to the right. However, the rotation is not so drastic as for terminal A. With the branch moved from the center of the main wire to 400 nm to the right and 700 nm to the right, the emission intensity at terminal C is increased gradually. As the branch wire is moved off the middle of the main wire, the distance that the generated SPs propagate over in the main wire is changed. As is known, the Ag nanowire behaves like a Fabry–Pérot cavity to selectively modulate the output at the terminals. The change of the output behavior for terminals A and C in the branch structure is probably caused by the Fabry–Pérot resonances of different SP modes. Fixing the radius of the main wire as 150 nm and varying the radius of the branch wire as 120 nm, 130 nm, and 140 nm, the corresponding incident polarization dependent intensity at the three output terminals is shown in Figs. 4(d)–4(f). The strongest emission of the branch also occurs when the incident polarization is parallel to its long axis. However, for terminals A and C, the output behavior becomes quite different. Since both the main wire and the branch wire are placed on the same glass substrate, the decrease of the branch wire radius changes the geometries of the junction, which influences the plasmon modes launched by gap-excitation and thus changes the output behavior.

In conclusion, we have investigated the controllable plasmon excitation in branched nanowire structures. From the results of both experiments and simulations, it is found that the detailed branched nanostructure geometries play an import role in determining the excitation of surface plasmons and thus the output. By controlling the polarization of the excitation light, the plasmons can be selectively launched to the branch wire or the main wire, which is related to the SP excitation manners. We study the SP excitation dependence on the branch angle, position of the junction along the main wire, and the radii of the nanowires. The controllable excitation of the propagating surface plasmons in the branched nanowire structures may be used for a selective SP launcher or addressable light splitter to be integrated into SP-based nanophotonic circuits.

We thank Li Chen for the help in preparing the manuscript.

References

[1] Xu H X, Bjerneld E J, Kall M and Borjesson L 1999 *Phys. Rev. Lett.* **83** 4357
[2] Xu H X, Aizpurua J, Kall M and Apell P 2000 *Phys. Rev.* E **62** 4318
[3] Mayer K M and Hafner J H 2011 *Chem. Rev.* **111** 3828
[4] Ma X, Xu X, Zheng Z, Wang K, Su Y, Fan J, Zhang R, Song L, Wang Z and Zhu J 2010 *Sens. Actuators A-Phys.* **157** 9
[5] Xu H X and Kall M 2002 *Phys. Rev. Lett.* **89** 246802
[6] Juan M L, Righini M and Quidant R 2011 *Nature Photon.* **5** 349
[7] Berini P and De Leon I 2012 *Nature Photon.* **6** 16
[8] Ozbay E 2006 *Science* **311** 189
[9] Fang Y R, Li Z P, Huang Y Z, Zhang S P, Nordlander P, Halas N J and Xu H X 2010 *Nano Lett.* **10** 1950
[10] Wei H, Li Z P, Tian X R, Wang Z X, Cong F Z, Liu N,

Zhang S P, Nordlander P, Halas N J and Xu H X 2011 *Nano Lett.* **11** 471
[11] Wei H, Wang Z X, Tian X R, Kall M and Xu H X 2011 *Nature Commun.* **2** 387
[12] Guo X, Qiu M, Bao J M, Wiley B J, Yang Q, Zhang X N, Ma Y G, Yu H K and Tong L M 2009 *Nano Lett.* **9** 4515
[13] Kim N C, Li J B, Yang Z J, Hao Z H and Wang Q Q 2010 *Appl. Phys. Lett.* **97** 061110
[14] Gonzalez-Tudela A, Martin-Cano D, Moreno E, Martin-Moreno L, Tejedor C and Garcia-Vidal F J 2011 *Phys. Rev. Lett.* **106** 020501
[15] Ditlbacher H, Hohenau A, Wagner D, Kreibig U, Rogers M, Hofer F, Aussenegg F R and Krenn J R 2005 *Phys. Rev. Lett.* **95** 257403
[16] Sanders A W, Routenberg D A, Wiley B J, Xia Y N, Dufresne E R and Reed M A 2006 *Nano Lett.* **6** 1822
[17] Knight M W, Grady N K, Bardhan R, Hao F, Nordlander P and Halas N J 2007 *Nano Lett.* **7** 2346
[18] Fang Y R, Wei H, Hao F, Nordlander P and Xu H X 2009 *Nano Lett.* **9** 2049
[19] Akimov A V, Mukherjee A, Yu C L, Chang D E, Zibrov A S, Hemmer P R, Park H and Lukin M D 2007 *Nature* **450** 402
[20] Wei H, Ratchford D, Li X Q, Xu H X and Shih C K 2009 *Nano Lett.* **9** 4168
[21] Kolesov R, Grotz B, Balasubramanian G, Stohr R J, Nicolet A A L, Hemmer P R, Jelezko F and Wrachtrup J 2009 *Nature Phys.* **5** 470
[22] Li Q, Wang S S, Chen Y T, Yan M, Tong L M and Qiu M 2011 *IEEE J. Sel. Top. Quantum Electron.* **17** 1107
[23] Li Z P, Hao F, Huang Y Z, Fang Y R, Nordlander P and Xu H X 2009 *Nano Lett.* **9** 4383
[24] Shegai T, Miljkovic V D, Bao K, Xu H X, Nordlander P, Johansson P and Kall M 2011 *Nano Lett.* **11** 706
[25] Li Z P, Bao K, Fang Y R, Huang Y Z, Nordlander P and Xu H X 2010 *Nano Lett.* **10** 1831
[26] Shegai T, Huang Y Z, Xu H X and Kall M 2010 *Appl. Phys. Lett.* **96** 103114
[27] Wang W H, Yang Q, Fan F R, Xu H X and Wang Z L 2011 *Nano Lett.* **11** 1603
[28] Li Z P, Bao K, Fang Y R, Guan Z Q, Halas N J, Nordlander P and Xu H X 2010 *Phys. Rev.* B **82** 241402
[29] Allione M, Temnov V V, Fedutik Y, Woggon U and Artemyev M V 2008 *Nano Lett.* **8** 31
[30] Rewitz C, Keitzl T, Tuchscherer P, Huang J, Geisler P, Razinskas G, Hecht B and Brixner T 2012 *Nano Lett.* **12** 45
[31] Li Z P, Zhang S P, Halas N J, Nordlander P and Xu H X 2011 *Small* **7** 593
[32] Sun Y G and Xia Y N 2002 *Adv. Mater.* **14** 833